Wideband Simultaneous Dual Circularly Polarized Phased Array Subarray with Scalable Characteristics for Satellite Communications

Yunqi Zhang, Jiateng Chen, Xuping Li, Rui Yang, Qizheng Zhao, Xueyan Song, and Wenjia Zhou

School of Electronic Engineering
Xi'an University of Posts & Telecommunications, Xi'an 710121, China
zhangyunqi@xupt.edu.cn, chenjiatengxian@163.com, lixuping@163.com, r18329386436@163.com, 201759789@qq.com, xysong6597@126.com, zhouwj1986@163.com

Abstract – This paper proposes a budget-friendly, highly integrated, and low-profile wideband simultaneous dual circularly polarized phased array subarray with scalable characteristics for satellite communications. In order to achieve wideband, the antenna unit is not only fed by double-fed point probe contact, but also by electromagnetic coupling. Moreover, the dual circularly polarized radiation of the antenna unit is realized by a miniaturized 3 dB bridge-type phase-shift network. In addition, the phased array subarray uses metalized vias to reduce inter-element crosstalk, which effectively improves the active voltage standing wave ratio (VSWR) and beam steering characteristics. Also, the subarray has interchangeability and versatility, enabling convenient two-dimensional expansion to form a tile-type phased array antenna. Besides, the phased array subarray can be used to achieve two-dimensional $\pm 40^{\circ}$ beam scanning in both the azimuth and elevation planes. Within $\pm 40^{\circ}$ beam scanning, the active VSWR of the subarray is less than 2.5 in 9.55 - 14.35 GHz (40.17%). At 12.1 GHz, the two-dimensional gain decreases by less than 2.1 dB and 1.95 dB, respectively. The proposed antenna exhibits good performance in terms of matching and beam steering characteristics, which make it suitable for use in future 5G/6G phased array antenna systems.

Index Terms – Modular, phased array, simultaneous dual circular polarization, wideband.

I. INTRODUCTION

Satellite communication presents a practical approach for worldwide coverage and universal connectivity. The Low-Earth orbit (LEO) satellites, operating in orbits ranging from 200 to 2000 km, necessitate continuous tracking. Thus, phased array technology that is affordable, highly integrated, and low-profile is desperately needed [1–3]. In addition, dual-circularly polarized antenna not only has the advantages of anti-attenuation and anti-multipath interference, but also the aperture efficiency can be improved and the capacity of the communication system can be increased [4–7].

The phased array antenna possesses the characteristics of flexible beam control, fast response speed, and high positioning accuracy [8]. Regrettably, the conventional large-scale phased array is typically built as a whole array, entailing an arduous design process. Also, it has high cost and is not easy to use and maintain. This restricts the comprehensive promotion and large-scale application of phased array technology.

In [9], a dual-circularly polarized antenna is composed of a dual-band monopole antenna and a polarization rotation artificial magnetic conductor (PRAMC). Its application scenarios and implementation forms are novel, yet not wide enough (about 10%). Also, the implementation of dual-circular polarization can also be viably achieved through the employment of PIN diodes, such as [10]. The antenna switches the long axis and short axis of the cross slot by changing the on/off state of the diode. This achieves a switch between left-hand circularly polarized (LHCP) and right-hand circularly polarized (RHCP), with a relative bandwidth of 27.6%. Nevertheless, the regulation of diodes necessitates the integration of supplementary biasing circuits. This not only compounds the intricacy of antenna design but also gives rise to electromagnetic compatibility (EMC) concerns. In addition, an antenna based on a small-size, low-profile, F-shaped waveguide slot circular polarizer is reported in [11]. The height of the circular polarizer is only 1/6 wavelength and the width is about 2/5 wavelength. For all that, the structure of the F-shaped circular polarizer is complex, the processing is difficult, and the relative bandwidth is less than 10%. The metasurface antennas, characterized by their beam-scanning properties and inherent benefits of affordability and ease of conformability, have emerged as a vigorously researched topic in current scientific investigations [12–14]. Also, the metasurface circular polarization patch

Submitted On: November 10, 2023
Accepted On: April 2, 2024

https://doi.org/10.13052/2024.ACES.J.390310

antenna phased arrays [15] were discussed, though the metasurface antenna requires an independent feed power to excite, and the overall profile size is high.

In this paper, a budget-friendly, highly integrated and low-profile wideband simultaneous dual circularly polarized phased array subarray with scalable characteristics is designed for satellite communication. The proposed antenna profile, characterized by a mere height of 0.15 λ_0 (free-space wavelength), operates within the Ku-band and is inherently conformal. By using frequency-division-multiple-access (FDMA) technology, LHCP wave and RHCP wave can be radiated simultaneously. The proposed antenna can significantly enhance the aperture efficiency, lower costs, and increase communication system capacity, making it suitable for future satellite communication applications. In addition, based on the modular phased array subarray with dual-circular polarization, the open and scalable design facilitates convenient two-dimensional expansion to form a tile-type phased array antenna.

II. PHASED ARRAY ANTENNA UNIT ANALYSIS AND DESIGN

The circular microstrip antenna works in the main mode TM_{01}, and the theoretical patch radius R of the circular microstrip antenna can be calculated to be 3.91 mm by theoretical empirical formulas (1) and (2). Meanwhile, considering the influence of parasitic patches, the specific size needs to be optimized and adjusted. The configuration of the phased array antenna unit optimized by multiple iterations is depicted in Fig. 1. The optimized process is from prototype 1 of single-stage 3 dB bridge network with single-layer microstrip patch to prototype 2 of multi-stage bridge phase-shifting network with single-layer microstrip patch, and then to the existing prototype 3 of miniaturized bridge phase-shifting network with double-layer microstrip patch.

$$R = \frac{K}{\left[1 + \frac{2h}{\pi\varepsilon_r K}\left\{\ln\left(\frac{\pi K}{2h}\right) + 1.7726\right\}\right]^{1/2}}. \quad (1)$$

$$K = \frac{87.94}{f_r\sqrt{\varepsilon_r}}. \quad (2)$$

f_r is the operating frequency (GHz), ε_r is the relative dielectric constant, and the unit of R is mm.

As shown in Figs. 1 (a) and (b), the antenna unit consists of five layers (layer 1, layer 2, layer3, phase-shifting network, and layer 4), which are printed on four square dielectric substrates and thickness are $Hsub_1$, $Hsub_2$, $Hsub_3$, $Hsub_4$. The use of thicker dielectric substrates 1 and 2 is effective for bandwidth expansion. Conversely, the selection of thinner dielectric substrates 3 and 4 serves to effectively reduce the width of low-impedance lines, thereby facilitating routing and miniaturization of the phase-shifting network. The substrates are RT/Duroid 5880 (ε_r = 2.2, tan δ = 0.0009).

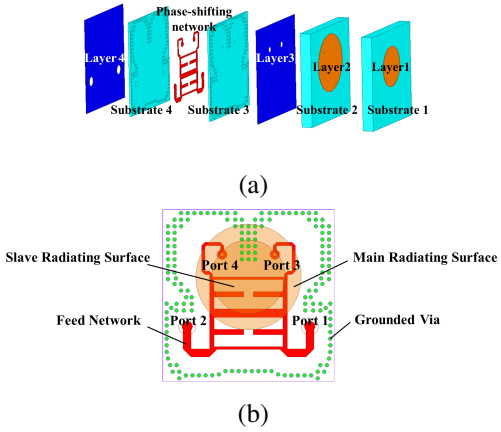

Fig. 1. Geometry of the proposed antenna unit: (a) 3D view and (b) perspective view.

Layers 1 and 2 are circular patches with different radii. As can be observed, layer 1 serves the function of bandwidth broadening and gain enhancement. A wideband 3 dB bridge miniaturized by T-type equivalent method composes the phase-shifting network, which is a stripline structure. The phase-shifting network and layer 2 are connected through a metalized vias. Layers 3 and 4 concurrently fulfill the dual role of serving as reflectors, thereby contributing to the reduction of backlobes in the antenna and simultaneously enhancing the gain of the main lobe.

Theoretically, the amplitude and phase difference required for circular polarization can be provided by the 3 dB bridge network through reasonable design. A phase difference of 90° and -90° exists between port 3 and port 4. When port 1 and port 2 are separately fed with power, the antenna unit correspondingly generates LHCP and RHCP. Ports 1 and 2 are independently connected, with the amplitudes and phases of the excitations generated by the antenna unit being actively controlled by the transmitter and receiver. If a signal with the same frequency as the LHCP port and the RHCP port is excited at the same time, a linear polarization (LP) wave will be synthesized. To achieve simultaneous dual circular polarization, frequency-division-multiple-access (FDMA) technology is employed, allowing signals of different frequencies to be simultaneously excited at both the LHCP port and the RHCP port.

The designed phase-shifting network is capable of stably delivering excitation signals across a wide bandwidth, as depicted in Fig. 2. Figure 2 (a) shows that the simulated -10 dB impedance bandwidth of phase-shifting network ranges from 8.3 to 14.7 GHz (55.7%).

Meanwhile, the insertion loss is less than 3.65 dB, and the difference between them is less than 0.8 dB from 8.8 to 15 GHz (52.1%). Furthermore, it can be seen from Fig. 2 (b) that the phase difference of the phase-shifting network falls within the range of 85.2° to 95.1°.

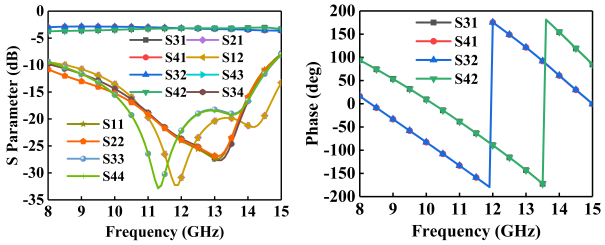

(a) (b)

Fig. 2. Results of phase-shifting network simulation: (a) S parameter and (b) phase.

In Fig. 3 (a), it is observed that the -10 dB impedance bandwidth of the antenna unit covers the range from 8.15 to 14.95 GHz (58.9%), exhibiting preferable matching and isolation characteristics. In addition, the majority frequency band demonstrates stable and high gain with low axial ratio (AR), as shown in Fig. 3 (b). It is noteworthy that the gain and axial ratio curves for LHCP and RHCP demonstrate a commendable level of consistency, an outcome attributed to the inherent high degree of symmetry in the proposed structure.

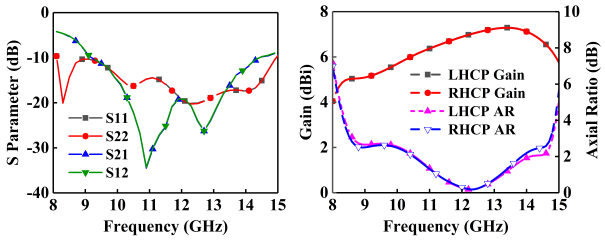

(a) (b)

Fig. 3. Simulation results of the phased array antenna unit: (a) S parameter and (b) gain and axial ratio.

III. ANALYSIS AND DESIGN OF MODULAR PHASED ARRAY SUBARRAYS

Moreover, a modular phased array subarray is developed by employing the aforementioned wideband dual circularly polarized antenna unit. The adoption of a modular design leads to reduced cable usage, thereby enhancing the reliability and maintainability of product. Upon the occurrence of a fault and subsequent identification of the problematic component, a swift replacement of the modular subarray serves as the remedy to rectify the issue.

The anticipated beam scanning range of the proposed antenna is ± 40°. Nevertheless, the presence of grating lobes not only diminishes antenna gain but also passively contributes to inaccurate assessments in target localization and direction finding. To prevent the emergence of grating lobes, formula (3) can be used to calculate the theoretical maximum inter-element spacing of 14.33 mm [16]. An ideal inter-element spacing would be 13 mm, taking into account different radiative indices like gain and grating lobe, as well as structural factors like feed network wiring.

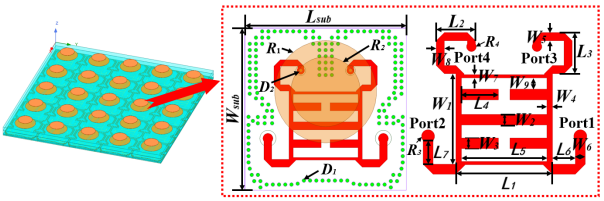

(a) (b)

Fig. 4. Modular phased array subarrays: (a) 3D view and (b) perspective view of the antenna unit and the optimized phase shift network.

Table 1: Optimized design parameters (in millimeters)

W_{sub}	13	R_1	4.10	L_4	2.25
W_1	5.47	R_2	2.80	L_5	5.21
W_2	0.65	R_3	0.4	L_6	1.38
W_3	0.65	R_4	0.34	L_7	1.44
W_4	0.35	D_1	0.3	$Hsub_1$	1.524
W_5	0.5	D_2	0.25	$Hsub_2$	1.524
W_6	0.62	L_{sub}	13	$Hsub_3$	0.254
W_7	0.2	L_1	5.90	$Hsub_4$	0.254
W_8	0.5	L_2	2.40		
W_9	0.78	L_3	2.49		

$$d \leq \frac{\lambda}{1+|\sin\theta_s|}. \tag{3}$$

λ is the wavelength and θ_s is the maximum scanning angle of the antenna.

The phased array subarray, as depicted in Fig. 4, is composed of the aforementioned antenna units. The optimized design parameters are shown in Table 1 of the antenna unit. The utilization of scalable concepts enables an easy expansion of the low-profile, wideband, dual-circularly polarized modular subarray into arbitrarily scaled tile-type two-dimensional phased array antennas.

Too small unit spacing will produce serious coupling phenomena. Also, the phase-shifting network with stripline structure is prone to resonance. To mitigate

coupling interference among individual antenna units, a cavity-like structure can be effectively established by strategically positioning metallized ground vias around the phase-shifting network and radiating elements. The active voltage standing wave ratio (VSWR) characteristics of wideband dual-circularly polarized modular phased array subarrays can be effectively improved through this approach. In addition, double-layered metallized ground vias can be strategically placed in certain regions to further reinforce the formation of a cavity-like structure for more effective suppression of coupling interference.

As shown in Fig. 5, it can be discerned that the modular phased array subarray exhibits commendable matching characteristics within a beam scanning range of $\pm 40^{\circ}$. The active VSWR in both the azimuth and elevation planes remains below 2.5 across a frequency range spanning from 9.55 to 14.35 GHz (40.17%). During two-dimensional scanning of the subarray, the gain decrease is observed to be less than 3.25 dB from 9.3 to 14.2 GHz. Among them, at 12.1 GHz, the gain reduction in the azimuth and elevation planes is less than 2.1 dB and 1.95 dB, respectively. From 10 to 14.2 GHz (34.71%), the AR of the two-dimensional scan performed by the subarray stays below 3 dB. The performance of the wideband, dual-circularly polarized modular phased array subarray, as evidenced by the presented data, passively demonstrates its excellence in maintaining consistent and stable radiation of circularly polarized waves.

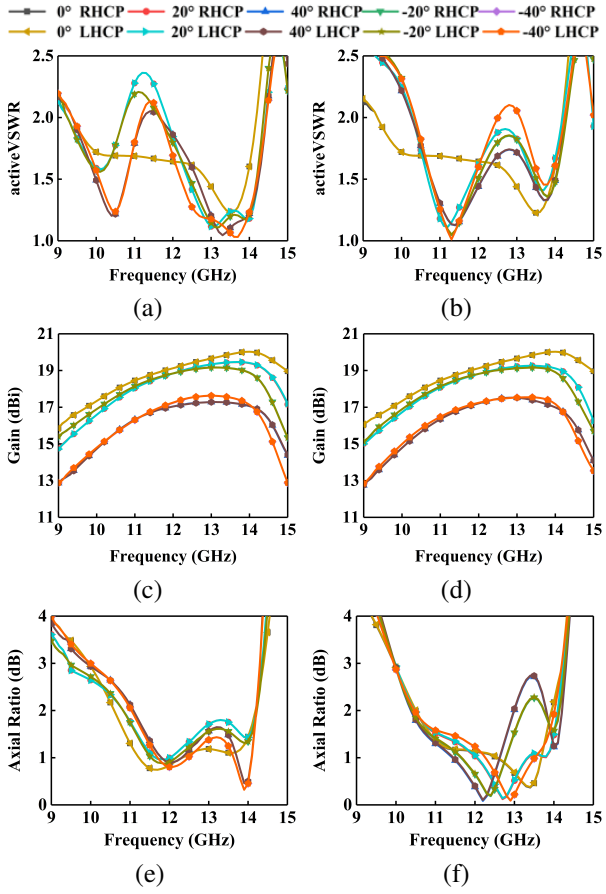

Fig. 5. Simulation results of the modular subarray: (a) Azimuth plane active standing wave, (b) elevation plane active standing wave, (c) azimuth plane gain, (d) elevation plane gain, (e) azimuth plane axial ratio, and (f) elevation plane axial ratio.

IV. PROCESS AND MEASUREMENT

To validate the effectiveness of the design proposed in this paper, the subarray of the modular phased array antenna was fabricated according to the dimensions provided in the preceding text. This includes 5×5 wideband dual circularly polarized phased array antenna elements. The picture of the processed subarray antenna and its measurement environment is presented in Fig. 6 (a). To verify the performance of the proposed antenna, a transmitter and receiver platform covering the Ku-band in Fig. 6 (b) is used. After determining the target scanning angle θ of antenna array, the phase difference φ is fed between the adjacent antenna units, and the beam of the array antenna can be scanned to the target scanning angle θ. Among them, the phase difference φ is calculated by formula (4), and provided by the phase shifter shown in Fig. 6 (b), and d is the antenna element spacing. If the target scanning angle θ is 30°, the unit spacing d is 13 mm, and the frequency f is 12.1 GHz, the phase difference φ can be calculated to be 94.38°. Other cases are similar.

$$\varphi = \frac{2\pi}{\lambda} d \sin\theta. \tag{4}$$

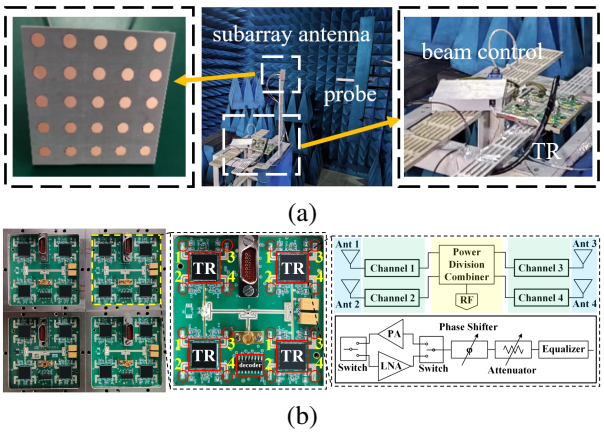

Fig. 6. Process and measure: (a) Processed of subarray antenna and measurement environment and (b) transmitter and receiver.

Table 2: Comparison between reported works and proposed antenna

Ref.	Type of Unit	Polar	Scanning Angle and Dimension	Size ($\lambda_0{}^3$)	AR Bandwidth (GHz)	Gain (dBic)	Impedance Bandwidth (GHz)	Diode
[9]	Monopole and PRAMC	Dual circular	1-D	0.72×0.72×0.06	3.5/5.8 (2%/8.2%)	6.6/ 7.2	3.5/5.8 (11.7%/9.1%)	No
[10]	Microstrip antenna	Dual circular	-	0.4×0.4×0.04	2.0-2.7 (29.8%)	5.95	1.97-2.72 (32%)	Yes
[11]	Waveguide slot antenna	Single circular	±60°/1-D	8×46.08×1.46	Ka (less than 10%)	35.9	Ka (less than 10%)	No
[12]	Metasurface antenna	Single circular	±42°/1-D	0.53×17.07×0.155	24.15-27.5 (13.4%)	19.3	22.5-27.5 (20%)	No
[15]	Metasurface antenna	Single circular	±30°/2-D	4.08×4.08	27.3-31.3 (13.65%)	-	28-31 (10.177%)	No
This work	Stacked microstrip antenna	Dual circular	±40°/2-D	15.73×15.73×0.15	10-14.2 (34.71%)	32.77	9.55-14.35 (40.17%)	No

Also, the antenna and the transmitter and receiver are connected by RF cables. Based on this subarray, the results of synthesizing an array composed of 6×6 such subarrays have been derived. Due to the large array size, the method based on the array factor approach was employed to measure the array factor of the center element of the modular phased array subarray for obtaining the scanning characteristics of the phased array beam. The radiation characteristics of a tile-type two-dimensional phased array antenna can be obtained by integrating the directional patterns of each element and gradually adjusting their phases using analysis software.

The measured normalized gain patterns in the azimuth and elevation planes for the central antenna unit are respectively presented in Figs. 7 (a) and (b), using the vector network analyzer Ceyear 3656D and the planar near-field microwave anechoic chamber for measurement. It can be discerned from Fig. 8 that the return loss

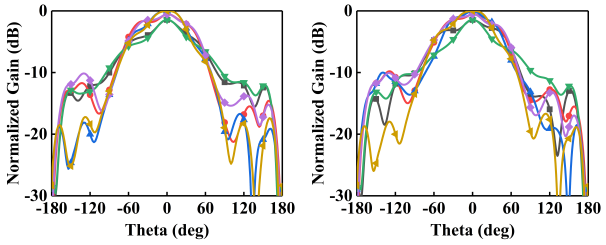

Fig. 7. (a) Azimuth plane measured unit normalized gain curve and (b) elevation plane measured unit normalized gain curve.

curves for the LHCP port and the RHCP port exhibit commendable consistency, with a -10 dB return loss bandwidth spanning from 9.5 to 14.3 GHz (40.34 %).

According to the measured radiation parameters of the antenna element in the array, the normalized gain scanning curve of the tiled two-dimensional phased array antenna can be obtained by using the pattern in the array [17], as shown in Figs. 9 and 10.

Furthermore, the gains of the scanning beams across the azimuthal and elevational dimensions are individually presented in Tables 3 and 4, respectively. It can be seen that the antenna exhibits good directionality and

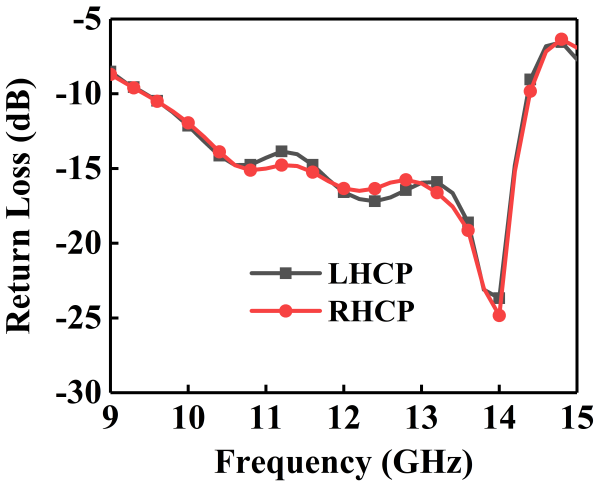

Fig. 8. Return loss of the central element of process of subarray antenna.

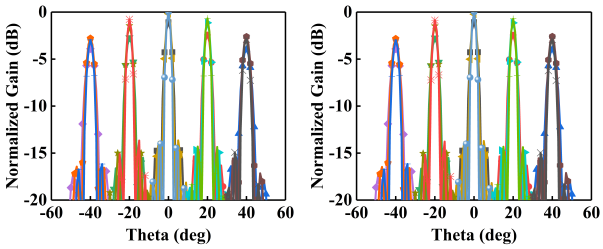

Fig. 9. Normalized gain scanning curves for azimuthal two-dimensional phased array antennas: (a) LHCP and (b) RHCP.

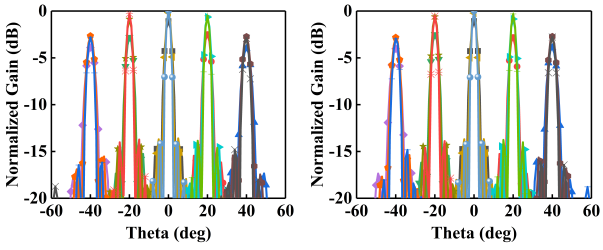

Fig. 10. Normalized gain scanning curves for elevating two-dimensional phased array antennas: (a) LHCP and (b) RHCP.

scanning characteristics, enabling phased scanning in the operational frequency range of $\pm 40^\circ$ in two dimensions.

The detailed performance comparison between the previously developed antenna prototype and the recently reported related works is presented in Table 2. In contrast to the monopole, PRAMC, microstrip and waveguide slot antenna in [9], [10], and [11], our prototype features wideband, simultaneously dual-circularly polarized, and scalable. Besides, compared with the metasurface antennas in [12] and [15], our prototype not only has almost the same or wider scanning range, but also achieves dual circular polarization. Most importantly, the prototype has a wider impedance bandwidth and axial ratio bandwidth,

Table 3: The gain of the scanning beam for azimuthal dimension (dBic)

S.A.*	Gain for Azimuthal Dimension LHCP/RHCP		
	10 GHz	12.1 GHz	14.2 GHz
-40°	28.03 / 28.09	30.71 / 30.7	30.69 / 30.86
-20°	29.65 / 29.52	31.69 / 31.67	32.17 / 32.05
0°	30.84 / 30.88	32.76 / 32.74	33.94 / 33.96
20°	29.51 / 29.49	31.8 / 31.85	32.26 / 32.23
40°	27.95 / 27.9	30.66 / 30.68	30.75 / 30.83

*: S.A. represents the beam scanning angle.

Table 4: The gain of the scanning beam for elevating dimension (dBic)

S.A.*	Gain for Elevating Dimension LHCP/RHCP		
	10 GHz	12.1 GHz	14.2 GHz
-40°	28.04 / 27.93	30.82 / 30.87	30.78 / 30.84
-20°	29.52 / 29.46	32.06 / 32.13	32.35 / 32.2
0°	30.85 / 30.89	32.77 / 32.73	33.93 / 33.91
20°	29.43 / 29.47	32.29 / 32.18	32.22 / 32.09
40°	27.94 / 28.02	30.91 / 30.86	31.01 / 30.96

*S.A. represents the beam scanning angle.

and its outstanding wideband performance is achieved in a compact size.

V. CONCLUSION

In this paper, a wideband simultaneous dual circularly polarized phased array subarray with scalable characteristics is designed for satellite communication. The subarray exhibits inherent advantages such as a wide operational bandwidth, dual-circular polarization capability, low profile, and ease of maintenance. It has interchangeability and versatility, allowing for rapid two-dimensional expansion and assembly into a tile-type phased array. This approach inherently enables the passive reduction of design complexity, enhancement of research and development efficiency, shortening of manufacturing cycles, and minimization of production costs. The wideband dual circularly polarized modular phased array subarray with excellent performance index is designed, simulated, fabricated and measured by using the wideband dual circularly polarized antenna unit. It can achieve two-dimensional $\pm 40^\circ$ phase-scanned scanning within a wide frequency band while radiating LHCP waves and RHCP waves simultaneously. Moreover, it possesses the characteristic of maintainability, such that upon the occurrence of a malfunction, once the fault location is swiftly identified, repair and replacement can promptly ensue. This has positive significance for engineering applications and aligns with the future trends of wideband, arrayed, versatile, and miniaturized phased array technology. It also has important application value in the fields of telemetry, reconnaissance and satellite communication.

ACKNOWLEDGMENT

This work is supported in part by Key Research and Development Program of Shaanxi (2021GY-049), Xi'an Science and Technology Plan Project (21XJZZ0071), Scientific Research Program Funded by Shaanxi Provincial Education Department (22JC058), Shanxi province science and technology department (2021ZDLGY08-03), and Natural Science Basic Research Program of Shaanxi (2022JQ-699).

REFERENCES

[1] G. Gültepe, T. Kanar, S. Zihir, and G. M. Rebeiz, "A 1024-element ku-band SATCOM phased-array transmitter with 45-dBW single-polarization EIRP," *IEEE Transactions on Microwave Theory and Techniques,* vol. 69, no.9, pp. 4157-4168, 2021.

[2] S. Rao, M. Tang, and C.-C. Hsu, "Multiple beam antenna technology for satellite communications payloads," *Applied Computational Electromagnetics (ACES) Journal*, vol. 21, no. 3, pp. 353-364, 2022.

[3] C.-N. Chen, Y.-H. Lin, L.-C. Hung, T.-C. Tang, W.-P. Chao, C.-Y. Chen, P.-H. Chuang, G.-Y. Lin, W.-J. Liao, Y.-H. Nien, and W.-C. Huang, "38-GHz phased array transmitter and receiver based on scalable phased array modules with endfire antenna arrays for 5G MMW data links," *IEEE Transactions on Microwave Theory and Techniques,* vol. 69, no. 1, pp. 980-999, 2021.

[4] L.-H. Ye, Y.-J. Li and D.-L. Wu, "Dual-wideband dual-polarized dipole antenna with t-shaped slots and stable radiation pattern," *IEEE Antennas and Wireless Propagation Letters*, vol. 21, no. 3, pp. 610-614, 2022.

[5] Q. Xu, S.-B Liu, Y.-X Wang, L. Song, and H. Cao, "Dual-polarized antenna based on printed dipole and microstrip patch," *Journal of Electronics & Information Technology*, vol. 39, no. 7, pp. 1764-1768, 2017.

[6] M. Kanagasabai, P. Sambandam, M. G. N. Alsath, S. Palaniswamy, A. Ravichandran, and C. Girinathan, "Miniaturized circularly polarized UWB antenna for body centric communication," *IEEE Transactions on Antennas and Propagation*, vol. 70, no. 1, pp. 189-196, 2022.

[7] Q.-C. Ye, J.-L. Li, and Y.-M. Zhang, "A circular polarization-reconfigurable antenna with enhanced axial ratio bandwidth," *IEEE Antennas and Wireless Propagation Letters*, vol. 21, no. 6, pp. 1248-1252, 2022.

[8] J. Zhang and H. Wu, "Simultaneous transmit and receive phased array system architecture and prototype comprehensive verification," *Applied Computational Electromagnetics (ACES) Journal*, vol. 37, no. 12, pp. 1257-1264, 2023.

[9] H.-C. Yang, X.-Y. Liu, Y. Fan, and L.-P. Xiong, "Dual-band textile antenna with dual circular polarizations using polarization rotation AMC for off-body communications," *IEEE Transactions on Antennas and Propagation*, vol. 70, no. 6, pp. 4189-4199, 2022.

[10] M. Li, Z.-H. Zhang, M.-C. Tang, L. Zhu, and N.-W. Liu, "Bandwidth enhancement and size reduction of a low-profile polarization-reconfigurable antenna by utilizing multiple resonances," *IEEE Transactions on Antennas and Propagation*, vol. 70, no. 2, pp. 1517-1522, 2022.

[11] B. Liu, S.-M. Gu, M.-X. Meng, K.-Y. Shi, K.-Q. Ding, L. Xu, Y.-T. Yang, and Y.-L. Chen, "A circularly polarized wide-scan waveguide slot phased array antenna with high efficiency for ka band application," *Journal of Electronics & Information Technology*, vol. 43, no. 6, pp. 1630-1636, 2021.

[12] Y.-S. Zhang, W. Hong, Z.-D. Ding, L. Yang, C. Zhu, and Y. Hu, "Circularly polarized metasurface phased array antenna system with wide axial-ratio beamwidth for LEO mobile satellite communication," *IEEE Transactions on Antennas and Propagation*, vol. 71, no. 6, pp. 4823-4833, 2023.

[13] S. Tiwari, A. K. Singh, A. K. Poddar, U. L. Rohde, and A. Dubey, "Active beamsteerable digital metasurface lens antenna for millimeter-wave applications," *IEEE Antennas and Wireless Propagation Letters (Early Access)*, 2023.

[14] C. Ni, Z.-K. Yu, L. Zhang, and Z.-X. Zhang, "A wide-band circularly polarized and beam deflection antenna based on two metasurfaces," *IEEE Antennas and Wireless Propagation Letters (Early Access)*, 2023.

[15] Z.-N. Chen, X.-M. Qing, X.-L. Tang, W. Liu, and R.-L. Xu, "Phased array metantennas for satellite communications," *IEEE Communications Magazine*, vol. 60, no. 1, pp. 46-50, 2022.

[16] C. A. Reddy, K. V. Janardhanan, K. K. Mukundan, and K. S. V. Shenoy, "Concept of an interlaced phased array for beam switching," *IEEE Transactions on Antennas and Propagation*, vol. 38, no. 4, pp. 573-575, 1990.

[17] D. M. Pozar, "A relation between the active input impedance and the active element pattern of a phased array," *IEEE Transactions on Antennas and Propagation*, vol. 51, no. 9, pp. 2486-2489, 2003.

Yunqi Zhang was born in Bao-Tou, Inner Mongolia, China. He received the master's degree and the Ph.D. degree in micro-electronics from Xidian University in 2012 and 2015, respectively. He is currently working in the Xi'an University of Posts & Telecommunications. His research interests include CP antennas, OAM, omnidirectional antennas, and phase array antennas.

Jiateng Chen is with the School of Electronic Engineering, Xi'an University of Posts & Telecommunications, Xi'an 710121, China. His main research interests include phased array antennas and CP antennas.

Xuping Li was born in Xi'an, Shanxi, China in 1981. He received the Ph.D. degree in electromagnetic fields and microwave technology from Xidian University, Xi'an, China, in 2015. His research interests are antenna theory and engineering.

Rui Yang is with the School of Electronic Engineering, Xi'an University of Posts & Telecommunications, Xi'an 710121, China. Her main research interests are array antennas and vortex electromagnetic waves.

Qizheng Zhao is with the School of Electronic Engineering, Xi'an University of Posts & Telecommunications, Xi'an 710121, China. His current research interests are signal processing and CP antennas.

Xueyan Song was born in Henan Province, China, 1989. She received the Ph.D. degree from Xidian University in 2018. Her research interests include artificial magnetic conductors, low RCS antennas, low-profile antennas, frequency selective surfaces, and reflector antennas.

Wenjia Zhou was born in Xi'an, Shanxi, China in 1986. She received the Ph.D. degree in control science and engineering from Northwestern Polytechnical University, Xi'an, China, in 2017. Her main research interests are antenna theory and engineering, and microwave signal delay and simulation.